2021 43rd Annual International Conference of the
IEEE Engineering in Medicine & Biology Society (EMBC)
Oct 31 - Nov 4, 2021. Virtual Conference

Spatial Feature Extraction of Vectorcardiography via Minimum Volume Ellipsoid Enclosure in Classifying Left Ventricular Hypertrophy

Yasuyuki Kataoka[1] and Hitonobu Tomoike[1]

Abstract— **The voltage criteria used to diagnose left ventricular hypertrophy (LVH) in the chest and limb leads are by no means absolute. In addition to QRS voltages, QRS axis and duration, and P wave characteristics, repolarization (ST-T) changes have been focused attention due to their representing left ventricular overload. Vectorcardiography (VCG) has been studied specifically on its repolarization abnormality. The present study aims to devise spatial feature extraction of VCG and assess it in the LVH classification task. A minimum volume ellipsoid enclosure was applied to six segments obtained from upstroke and downstroke of each P, QRS, and T loops of a single-beat VCG. For the evaluation, VCG and 12 lead ECG dataset along with LVH labels of 61 subjects were derived from public open data, PTB-XL. These classification performances were compared with the LVH diagnosis criteria in the standard 12 lead ECG. As a result, the Random Forest classifier trained by the proposed spatial VCG feature resulted in accuracy of 0.904 (95% confidence interval: 0.861-0.947) when the class-balanced dataset was evaluated, which slightly exceeded the feature of 12 lead ECG. The feature importance analysis provided the quantitative ranking of the spatial feature of VCG, which were practically similar to those of ECG in the LVH classification task. Since the VCG are spatially comparable with three-dimensional data of CT, MRI, or Echocardiography, VCG will shed light on the spatial behavior of electrical depolarization and repolarization abnormalities in cardiac diseases.**

I. INTRODUCTION

Heart problems such as high blood pressure, diabetes, valvular heart disease like stenosis or regurgitation, arrhythmias, enlargement of the aorta accompany left ventricular hypertrophy (LVH). LVH develops silently over several years without symptoms and can lead to severe problems such as heart failure, sudden cardiac death and, ischemic stroke. A routine ECG is used for diagnosing LVH.

The clinical studies have shown that Vectorcardiography (VCG) is advantageous over ECG signal analysis for detecting repolarization variability [1], myocardial injury after coronary surgery [2] or the cardiological diagnosis in general repolarization abnormality [3]. However, for the LVH diagnosis, there has also been a longstanding disagreement as to whether the ECG or VCG spaces appear as more informative, with reports showing the VCG as better [3], [4], similar [5] or, poorer [6] than the ECG.

A VCG depicts the orientation and strength of a single cardiac vector representing overall cardiac activity throughout the cardiac cycle in orthogonal three-dimensional space. Bonomini et al. [7] studied these VCG features in the transverse and frontal planes to construct LVH indexes and compared their diagnostic performance in the ECG and VCG spaces. Hasan et al. [1] surveyed VCG features such as *total cosine R to T*, *loop area*, or *azimuth and elevation*. Nevertheless, these approaches are not successful to elucidate diagnostic features of VCG. By nature, a VCG contains spatial features not observable in the standard 12 lead ECG. For example, each wave of P, ORS, or T is not symmetrical in any of the scaler ECG waveforms. Such characteristics may relate to action potential waveform as well as the three-dimensional complicated structure of the heart.

This study aims to quantify three-dimensional characteristics of P, QRS, and T loops in VCG, and such analysis may shed light on electrical propagations characteristic of the LVH. To view spatial characteristics of P, QRS, and T loops, a feature extraction method using minimum volume ellipsoid enclosure (MVEE) was applied to six segments of a single-beat VCG which are upstroke and downstroke of each P, QRS, and T loop. To train and evaluate the classification model, VCG and 12 lead ECG dataset with left LVH labels were collected from PTB-XL. Our results showed the performance difference in two different features: the proposed spatial VCG and the standard 12 lead ECG criterion for LVH classification. The trained model was analyzed by feature importance to find and validate the clinical relevance between the spatial features of VCG and LVH.

TABLE I: Two Datasets with LVH Labeled Data

Dataset Name	Class Ratio(LVH:normal)	Total Subjects
LVH_122	1:1	122
LVH_366	1:5	366

TABLE II: Description of Six Segmentation

Segment Name	Description
$seg\ p_1$	P wave onset to P wave peak
$seg\ p_2$	P wave peak to P wave offset
$seg\ r_1$	QRS complex onset to R peak
$seg\ r_2$	R peak to QRS complex offset
$seg\ t_1$	T wave onset to T peak
$seg\ t_2$	T peak to T wave offset

II. METHODS

A. Dataset

The target dataset was collected from PTB-XL in PhysioNet. [8], [9] The open dataset includes heart disease labels and standard 12 lead ECG for 10 seconds from a subject at 500[Hz]. In this study, a single heartbeat was considered as a sample, resulting in approximately 10 data samples from a subject.

[1]Yasuyuki Kataoka and Hitonobu Tomoike are with NTT Research, Inc., 940 Stewart Dr, Sunnyvale, 94085, CA, USA yasuyuki.kataoka@ntt-research.com, hitonobu.tomoike@ntt-research.com

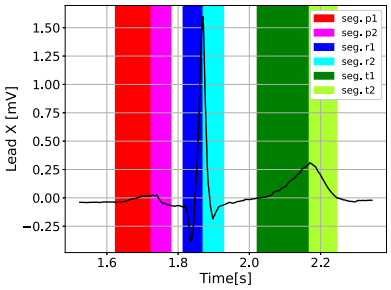

Fig. 1: Six segmentation on the ECG lead X of VCG

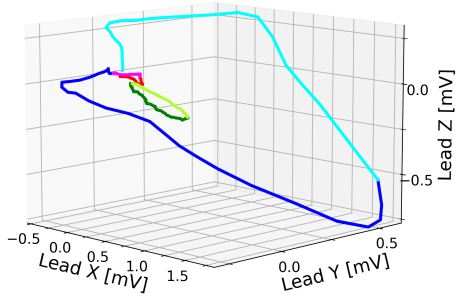

Fig. 2: Six segmentation on VCG

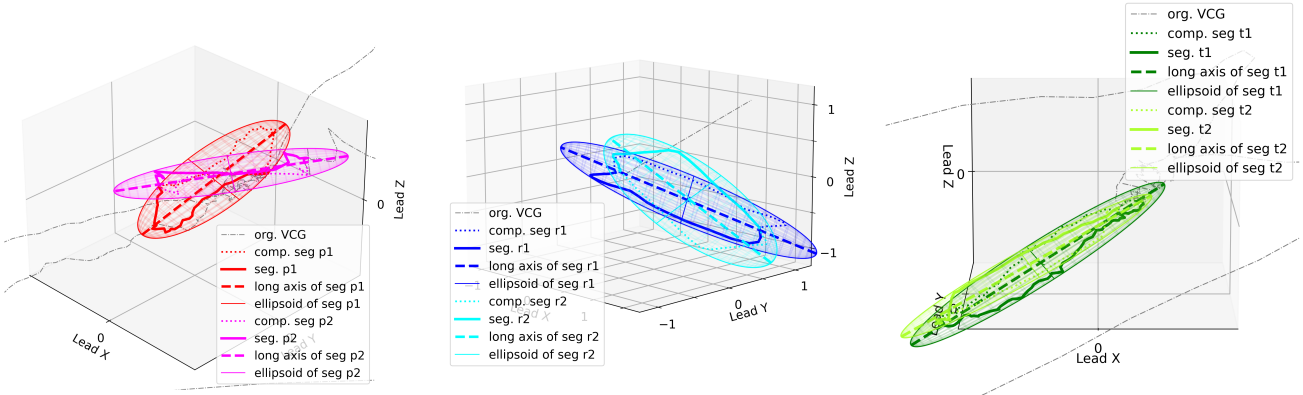

(a) P wave loop: $seg\ p_1$ and p_2 (b) QRS Complex loop: $seg\ r_1$ and r_2 (c) T wave loop: $seg\ t_1$ and t_2

Fig. 3: A sample of the proposed spatial feature of VCG via minimum volume enclosing ellipsoid to six segments

First, VCG was derived from 12 lead ECG using *Kors regression transformation* which was reported as the most accurate VCG approximation among five different transformation methods. [10]

Next, the labeled data of *LVH* and *normal* were selected by filtering PTBXL as follows. The *LVH* labeled data, 100% *LVH* and 0% for the other types, were selected. Likewise, the *normal* labeled data were selected, which has only 100% *normal* for the label. Both labeled data were also limited to the data verified by at least one cardiologist. The above process filtered the original dataset into 61 subjects with the *LVH* label and 5874 subjects with the *normal* label.

This class ratio of the obtained labeled data is highly imbalanced. Concerning the imbalanced class which badly affects the performance of machine learning, two undersampled datasets were derived for evaluation in this study as shown in Table. I. The undersampled data were chosen randomly.

B. Proposed Feature Extraction

The proposed spatial features are a total of 81 spatial features from a single-beat VCG.

1) Segmentation: VCG represents the three primal ECG waveforms (P wave, QRS complex, and T wave) as loop-shaped sequences in three-dimensional space. Based on the observation of each loop, the spatial morphologies are asymmetrical. This is because the first half and the second half of each loop are derived from different heart activities. For an example of P wave, the electrical signal begins in the sinoatrial node which is located in the right atrium and, travels to the right and left atria, causing them to contract and pump blood into the ventricles. Because of this asymmetric phenomenon, the loop of P wave can become asymmetric by its nature.

Accordingly, our proposed method divides each of the waves into two parts before and after the peak value as shown in Table. II. The detection algorithm for offset and peak points is the wavelet transform method against the lead X which is equivalent to the lead I. [11] Each wave composes a loop in three-dimensional space, meaning the onset point should be close to the offset point in the three-dimensional space. Thus, the onset value should be determined by the least euclidian distance to the offset value. The least euclidian distance is searched in the range $[\alpha, \beta]$ where β = (the time t at the peak value), $\alpha = (\beta - 2\Delta)$, Δ = (the time t of offset - β). An example of this segmentation method is shown in Fig.1 and Fig. 2,

2) Spatial Feature Computation: The MVEE [12] is applied to each segment for extracting the spatial features as shown in Fig. 3.

First, the half loop of each segment is virtually complemented for making it a complete loop. Because the original trajectory of each segment is a half loop, applying an ellipsoid enclosure to the original data points causes misfitting. Thus, the preprocessing is applied by adding virtual points that are origin symmetric points to the original data points in the segment. The virtual points for each segment are shown by dots in Fig. 3.

Second, MVEE is applied to each segment to computes the

ellipsoid that encloses N points in a D-dimensional space. In the case of our study, N is the data points of the sum of the original VCG and the complemented VCG, and D is three.

Third, the two types of spatial features, the rigid transformation and the ellipsoid shape, are extracted from a single estimated ellipsoid. The rigid transformation is composed of positional and postural transformation. The positional feature is given by the center coordinates $(x, y, z) \in \mathbb{R}(3)$ of the estimated ellipsoid. This represents the average voltage within the segment. The postural information is given by the rotation matrix of the ellipsoid. The postural feature, $(roll, pitch, yaw) \in \mathbb{S}(3)$ angles, can be computed from the rotation matrix. The ellipsoid shape is the components of ellipsoid such as the three axes, the maximum area, and the volume of the estimated ellipsoid. Adding them up, 11 features are computed for each segment.

Finally, the relative angles between the longest axes of the estimated ellipsoids are computed. The six ellipsoids provide 15 relatives angles by taking the combinations from them.

C. Evaluation

1) Machine Learning and Interpretation: The machine learning model was trained using the dataset and the proposed features for LVH classification problems. In our methods, the classifier was selected as a tree-based classifier, *Random Forest*. [13] Tree-based machine learning methods are based on decision trees built by recursively splitting a training sample, using different features from a dataset at each node that splits the data most effectively. These unique characteristics of the tree-based method enable model interpretation via feature importance, which is calculated as the decrease in node impurity, how well the trees split the data, weighted by the probability of reaching that node. The node probability or feature importance can be calculated by the number of samples that reach the node, divided by the total number of samples.

2) Data Split: The dataset is split into training set, development set, and test set by not the sample ID but the subject ID. First, the dataset was divided into test data and the other data by 10 fold stratified cross-validation. Then, the other data were divided into training data and development data by 5 fold stratified cross-validation. Using this data split, the nested cross-validation was conducted: the former split was used for the outer loop while the latter split was used for the inner loop. Among the five of trainings in the inner loop, hyperparameter tuning was held by grid search in a single training process using training and development sets. Then the best performing parameter among five trials was chosen for evaluating the performance on test data. The outer loop repeats the inner loop process ten times. Then, the overall performance was computed by ten of the test performances.

3) 12 lead ECG feature for comparison: To compare the proposed spatial features of VCG to another feature in the LVH classification task, this study adopted the features based on the diagnostic criteria of LVH using a standard 12 lead ECG. The diagnostic criteria include amplitude and temporal

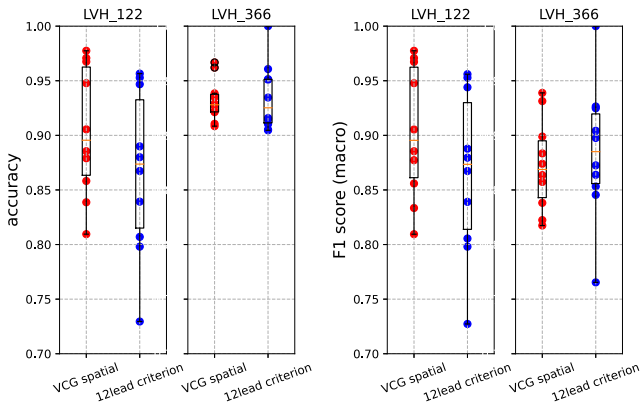

Fig. 4: Classification Performance: VCG vs 12 lead ECG

information, such as voltage criterion and QRS duration in specific leads. [14] Of all 47 feature candidates, only one feature was excluded, which was based on the non-trivial pointing system. Thus, a total of 46 feature values were calculated for each sample data. In the practice using diagnostic criteria, the LVH is judged by whether or not the value of each feature exceeds the threshold, but in our study, the feature is not binarized. This is because *Random Forest* can learn such a threshold from the data, so the keeping original value (float) should provide better performance.

III. Results

A. Classification Performance

The results of LVH classification on the test dataset is shown in Fig. 4. The outliers were determined if the result was outside of the range of 1.5 times the interquartile range above the upper quartile and below the lower quartile.

In evaluating LVH_122 with 95% confidence interval, the average accuracy and the macro average F1 score resulte in 0.904 (CI: 0.861-0.947) and 0.903 (CI: 0.860-0.946) for the proposed VCG spatial feature, and 0.867 (CI: 0.813-0.920) and 0.866 (CI: 0.812-0.919) for the 12 lead ECG feature. Likewise, in LVH_366, the the average accuracy and the macro average F1 score are 0.932 (CI: 0.918-0.946) and 0.872 (CI: 0.838-0.906) for the proposed VCG spatial feature, and 0.935 (CI: 0.913-0.957) and 0.885 (CI: 0.826-0.943) for the 12 lead ECG feature. The statistical significance was not recognized due to the high variance.

B. Feature Importance for LVH Classification

The top-ranked 30 of feature importances of the trained *Random Forest* using LVH_366 data are shown in Fig.5.

IV. Discussion

Since the test performance varied widely, it is difficult to conclude whether our proposed VCG spatial feature is superior or inferior to the standard 12 lead ECG criterion in the LVH classification task. This may be caused by the small number of LVH patients in the dataset. In our evaluation using 10-fold cross-validation, only about 6 subjects with LVH were included in a test set. Additional data collection of the labeled data of LVH is required to further study.

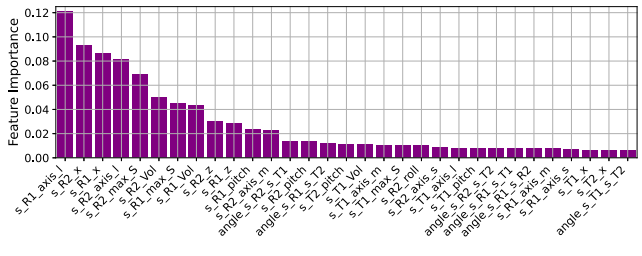

(a) Proposed VCG spatial features

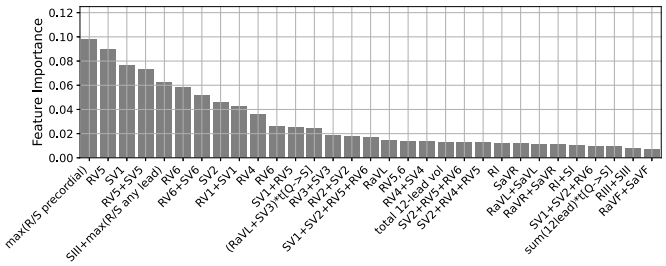

(b) Standard 12 lead ECG criterion for LVH diagnosis

Fig. 5: Top 30 feature importance of the trained models for Left Ventricular Hyptertrophy classification

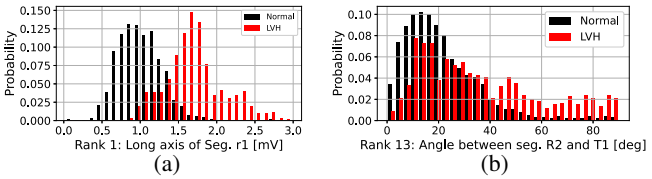

(a) (b)

Fig. 6: Distribution of features in LVH vs normal labels

In a recent paper on LVH classification where the class ratio of the labeled dataset is almost 1:1, a simple machine learning model has shown 71.4% accuracy using standard 12 lead ECG features. [15] This performance difference to our results should not be negligible. One of the potential reasons is that this study excluded the labels of complications, which clears the hyperplane of the classifier. We intentionally filtered the data to obtain higher accuracy in classification, to make our feature importance analysis more sense.

The feature importance shown in Fig. 5 revealed the ranking of the spatial feature of VCG and standard 12 lead ECG criterion in classifying LVH. The Fig. 6-(a) confirms the 1st ranked feature among VCG spatial features has a great difference in its distribution. The result also showed asymmetric results that $seg\ r_1$ is about 1.5 times more important than $seg\ r_2$. The relative angle between QRS complex and T wave loopwere ranked higher than all the other features of relative angles. Although these angles are well-known feature to detect LVH, the distribution of the angle between $seg\ r_1$ and $seg\ t_2$ shown in Fig. 6-(b) are less different than the feature of QRS complex.

V. Conclusion

This paper proposed the method to extract the spatial feature of VCG by aplying MVEE to six segments of a single-beat VCG which is composed of three asymmetrical loops. Our proposed feature extraction was compared to 12 lead ECG in the LVH diagnosis task. Then, our method clarified the ranking of diagnostic criteria for spatial features of VCG. The result confirmed that the spatial features of QRS complex are more dominant than other VCG spatial features in classifying LVH. Our overall proposed methods can be applied to different type of cardiac disease classification tasks to quantify the clinical relevance between the spatial feature of VCG and other cardiac disease type.

References

[1] Muhammad A Hasan and Derek Abbott. A review of beat-to-beat vectorcardiographic (VCG) parameters for analyzing repolarization variability in ECG signals. *Biomedizinische Technik. Biomedical engineering*, 61(1):3–17, feb 2016.

[2] L G Dahlin, C Ebeling-Barbier, E Nylander, H Rutberg, and R Svedjeholm. Vectorcardiography is superior to conventional ECG for detection of myocardial injury after coronary surgery. *Scandinavian cardiovascular journal : SCJ*, 35(2):125–128, mar 2001.

[3] Andrés Ricardo Pérez Riera, Augusto H Uchida, Celso Ferreira Filho, Adriano Meneghini, Celso Ferreira, Edgardo Schapacknik, Sergio Dubner, and Paulo Moffa. Significance of vectorcardiogram in the cardiological diagnosis of the 21st century. *Clinical cardiology*, 30(7):319–323, jul 2007.

[4] J.David Bristow. A study of the normal Frank vectorcardiogram. *American Heart Journal*, 61(2):242–249, 1961.

[5] ROMHILT DONALD W., GREENFIELD JOSEPH C., and ESTES E HARVEY. Vectorcardiographic Diagnosis of Left Ventricular Hypertrophy. *Circulation*, 37(1):15–19, jan 1968.

[6] E.Raymond Borun, John M Chapman, and Frank J Massey. Electrocardiographic data recorded with Frank leads: In subjects without cardiac disease and those with left ventricular overload. *The American Journal of Cardiology*, 18(5):656–663, 1966.

[7] Maria Paula Bonomini, Fernando Juan Ingallina, Valeria Barone, Ricardo Antonucci, Max Valentinuzzi, and Pedro David Arini. Left ventricular hypertrophy index based on a combination of frontal and transverse planes in the ECG and VCG: Diagnostic utility of cardiac vectors. *Journal of Physics: Conference Series*, 705:12031, 2016.

[8] Patrick Wagner, Nils Strodthoff, Ralf-Dieter Bousseljot, Dieter Kreiseler, Fatima I Lunze, Wojciech Samek, and Tobias Schaeffter. PTB-XL, a large publicly available electrocardiography dataset. *Scientific Data*, 7(1):154, 2020.

[9] Ary L Goldberger, Luis AN Amaral, Leon Glass, Jeffrey M Hausdorff, Plamen Ch Ivanov, Roger G Mark, Joseph E Mietus, George B Moody, Chung-Kang Peng, and H Eugene Stanley. Physiobank, physiotoolkit, and physionet: components of a new research resource for complex physiologic signals. *circulation*, 101(23):e215–e220, 2000.

[10] Rene Jaros, Radek Martinek, and Lukas Danys. Comparison of different electrocardiography with vectorcardiography transformations. *Sensors*, 19(14):3072, 2019.

[11] J P Martinez, R Almeida, S Olmos, A P Rocha, and P Laguna. A wavelet-based ECG delineator: evaluation on standard databases. *IEEE Transactions on Biomedical Engineering*, 51(4):570–581, apr 2004.

[12] Stefan Van Aelst and Peter Rousseeuw. Minimum Volume Ellipsoid. *Wiley Interdisciplinary Reviews: Computational Statistics*, 1:71–82, jul 2009.

[13] Yanjun Qi. Random Forest for Bioinformatics BT - Ensemble Machine Learning: Methods and Applications. pages 307–323. Springer US, Boston, MA, 2012.

[14] E William Hancock, Barbara J Deal, David M Mirvis, Peter Okin, Paul Kligfield, and Leonard S Gettes. Aha/accf/hrs recommendations for the standardization and interpretation of the electrocardiogram: Part v: electrocardiogram changes associated with cardiac chamber hypertrophy a scientific statement from the american heart association electrocardiography and arrhythmias committee, council on clinical cardiology; the american college of cardiology foundation; and the heart rhythm society endorsed by the international society for computerized electrocardiology. *Journal of the American College of Cardiology*, 53(11):992–1002, 2009.

[15] Fernando De la Garza-Salazar, Maria Elena Romero-Ibarguengoitia, Elias Abraham Rodriguez-Diaz, Jose Ramón Azpiri-Lopez, and Arnulfo González-Cantu. Improvement of electrocardiographic diagnostic accuracy of left ventricular hypertrophy using a Machine Learning approach. *PLOS ONE*, 15(5):e0232657, may 2020.